Numerical Analysis of the DoA estimation through BCS

M.Carlin, P. Rocca, G. Oliveri, and A. Massa

Abstract

This report deals with the Direction of arrival (DoA) estimation problem formulated within the Bayesian Compressive Sensing (BCS) framework. The performances of a novel method that directly works on the voltages measured at the output of the array elements without requiring the computation of the covariance matrix and that provide accurate and reliable DoAs estimation also without the a-priori knowledge on the number of incident signals have been investigated. The effectiveness of the proposed approach is assessed through an extensive numerical analysis addressing different scenarios, signal configurations, and noise conditions.

Estimation examples

$L = 2,\ SNR = 2\ dB$

$\widetilde{L} = L$

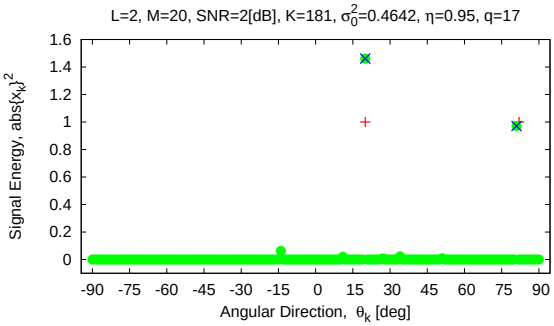

(a) $RMSE_\theta = 0.71\ \ [deg]$

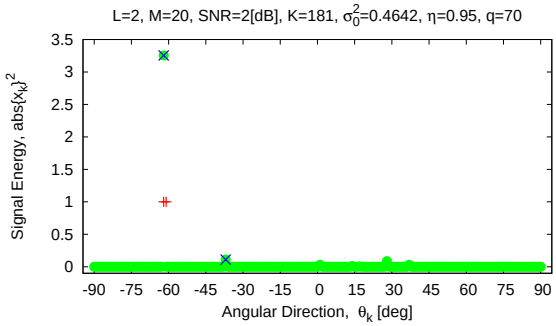

(b) $RMSE_\theta = 16.97\ \ [deg]$

$\widetilde{L} > L$

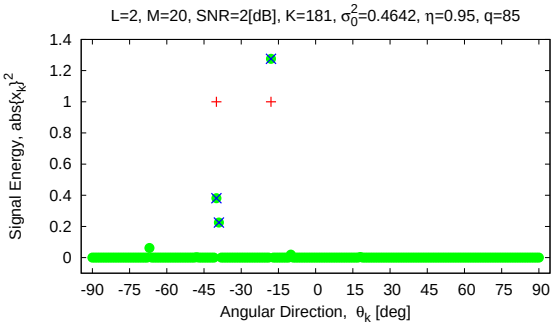

(c) $RMSE_\theta = 0.71\ \ [deg]$

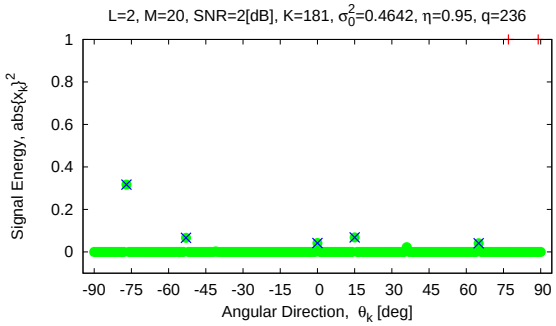

(d) $RMSE_\theta = 161.50\ \ [deg]$

$\widetilde{L} < L$

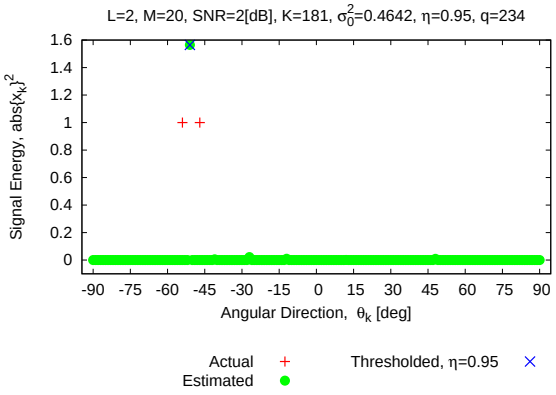

(e) $RMSE_\theta = 127.30\ \ [deg]$

Figure 1: *BCS DoA estimation examples*: (a) $\widetilde{L} = L$ with low $RMSE_\theta$, (b) $\widetilde{L} = L$ with high $RMSE_\theta$, (c) $\widetilde{L} > L$ with low $RMSE_\theta$, (d) $\widetilde{L} > L$ with high $RMSE_\theta$ and (e) $\widetilde{L} < L$ with high $RMSE_\theta$ (in this case it is impossible to obtain a low $RMSE_\theta$).

$L = 2,\ SNR = 10\ dB$

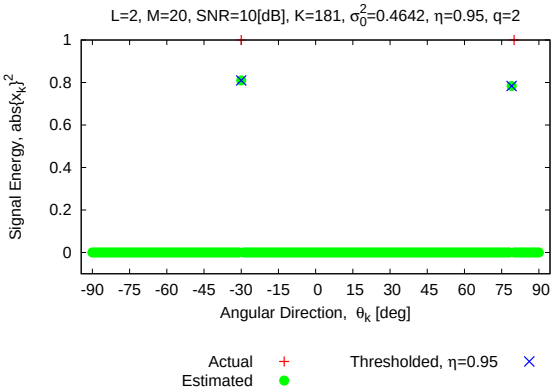

$\widetilde{L} = L$

(a) $RMSE_\theta = 0.71\ \ [deg]$

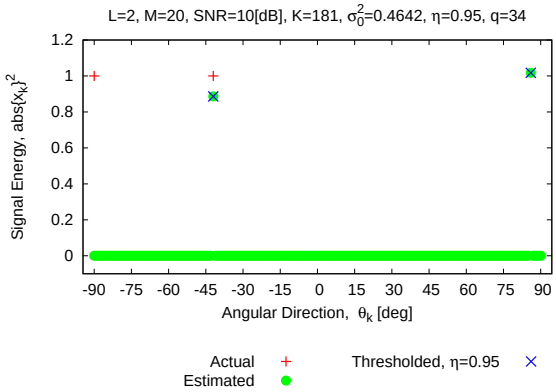

(b) $RMSE_\theta = 96.66\ \ [deg]$

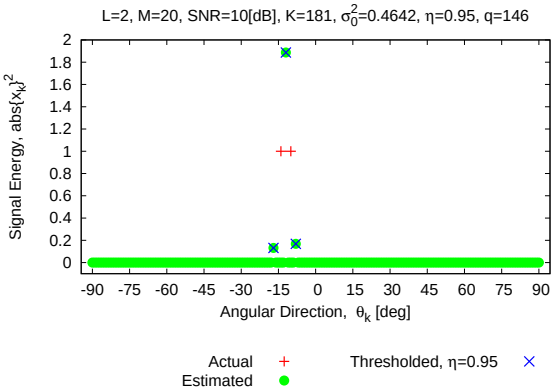

$\widetilde{L} > L$

(c) $RMSE_\theta = 2.92\ \ [deg]$

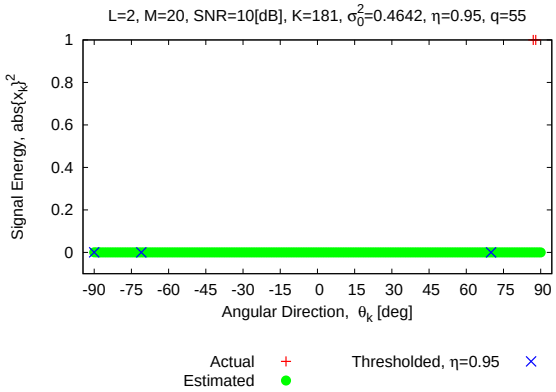

(d) $RMSE_\theta = 168.67\ \ [deg]$

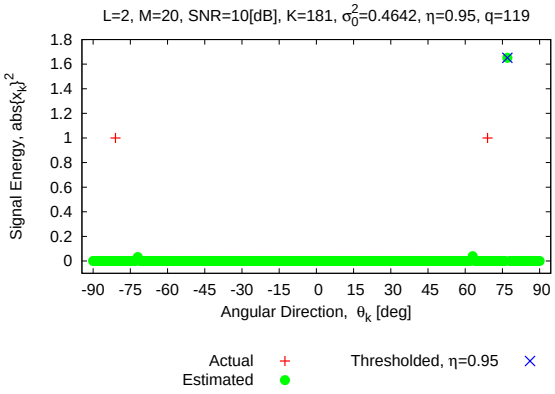

$\widetilde{L} < L$

(e) $RMSE_\theta = 127.41\ \ [deg]$

Figure 2: *BCS DoA estimation examples*: (a) $\widetilde{L} = L$ with low $RMSE_\theta$, (b) $\widetilde{L} = L$ with high $RMSE_\theta$, (c) $\widetilde{L} > L$ with low $RMSE_\theta$, (d) $\widetilde{L} > L$ with high $RMSE_\theta$ and (e) $\widetilde{L} < L$ with high $RMSE_\theta$ (in this case it is impossible to obtain a low $RMSE_\theta$).

$L = 4,\ SNR = 2\ dB$

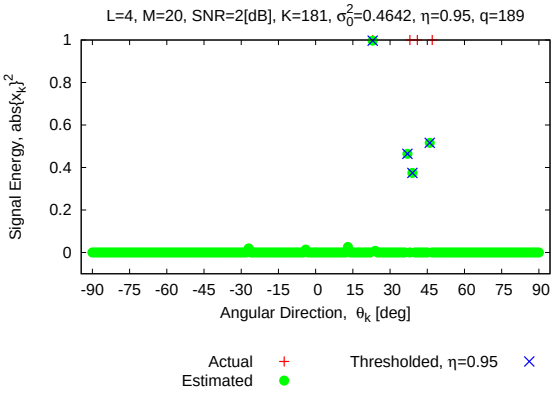

$\widetilde{L} = L$

(a) $RMSE_\theta = 1.22\,[deg]$

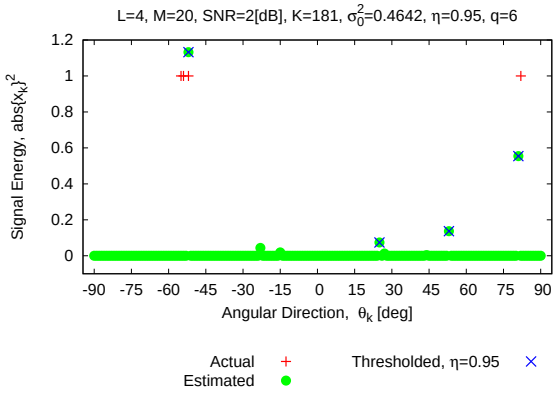

(b) $RMSE_\theta = 66.01\ \ [deg]$

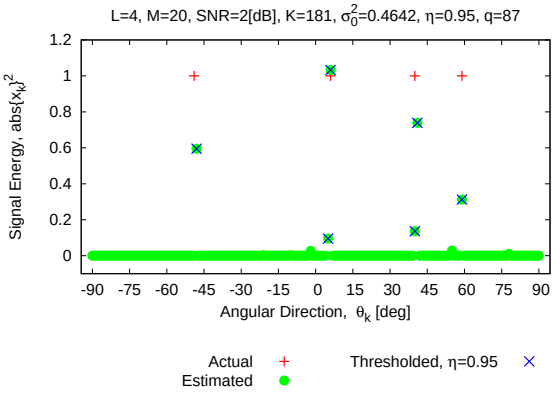

$\widetilde{L} > L$

(c) $RMSE_\theta = 0.87\ \ [deg]$

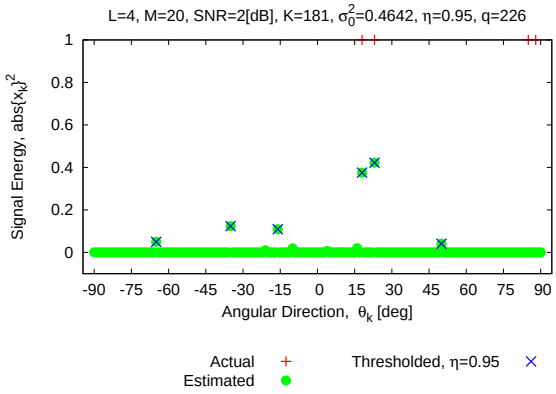

(d) $RMSE_\theta = 73.72\ \ [deg]$

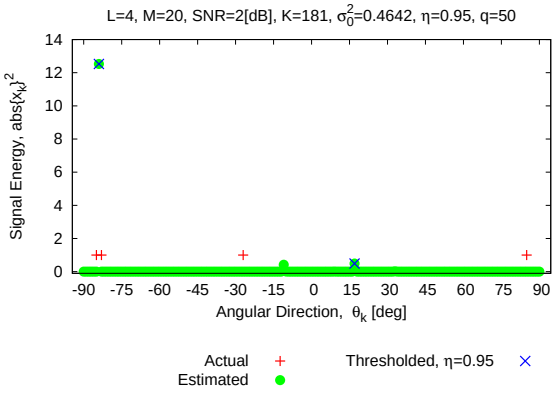

$\widetilde{L} < L$

(e) $RMSE_\theta = 129.17\ \ [deg]$

Figure 3: *BCS DoA estimation examples*: (a) $\widetilde{L} = L$ with low $RMSE_\theta$, (b) $\widetilde{L} = L$ with high $RMSE_\theta$, (c) $\widetilde{L} > L$ with low $RMSE_\theta$, (d) $\widetilde{L} > L$ with high $RMSE_\theta$ and (e) $\widetilde{L} < L$ with high $RMSE_\theta$ (in this case it is impossible to obtain a low $RMSE_\theta$).

$L = 4,\ SNR = 10\ dB$

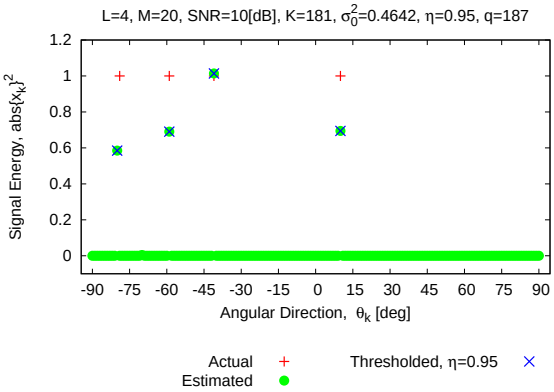

$\widetilde{L} = L$

(a) $RMSE_\theta = 0.50\ \ [deg]$

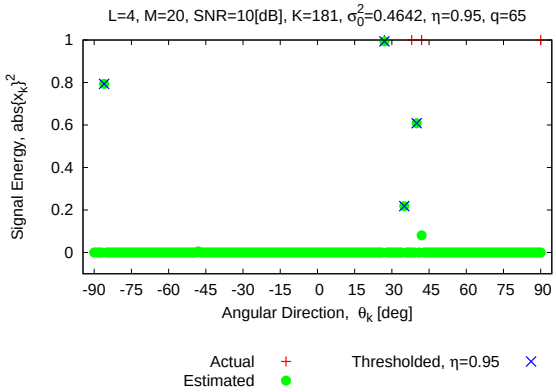

(b) $RMSE_\theta = 62.13\ \ [deg]$

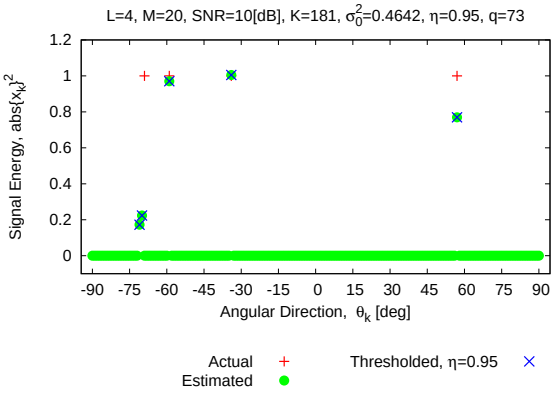

$\widetilde{L} > L$

(c) $RMSE_\theta = 1.12\ \ [deg]$

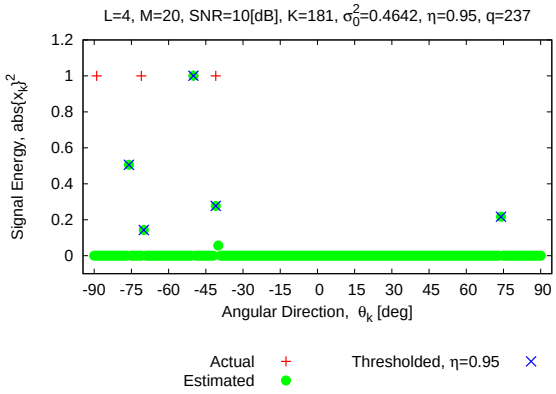

(d) $RMSE_\theta = 57.87\ \ [deg]$

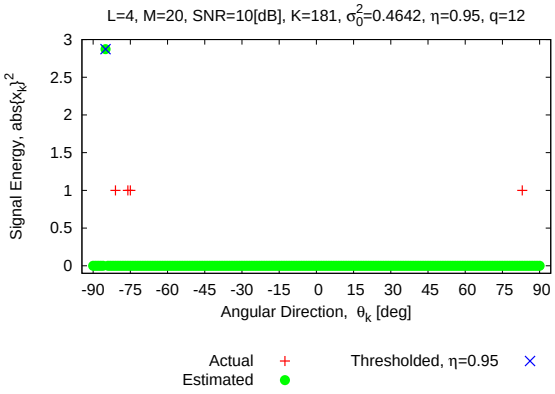

$\widetilde{L} < L$

(e) $RMSE_\theta = 155.90\ \ [deg]$

Figure 4: *BCS DoA estimation examples*: (a) $\widetilde{L} = L$ with low $RMSE_\theta$, (b) $\widetilde{L} = L$ with high $RMSE_\theta$, (c) $\widetilde{L} > L$ with low $RMSE_\theta$, (d) $\widetilde{L} > L$ with high $RMSE_\theta$ and (e) $\widetilde{L} < L$ with high $RMSE_\theta$ (in this case it is impossible to obtain a low $RMSE_\theta$).

$L = 6,\ SNR = 2\ dB$

$\widetilde{L} = L$

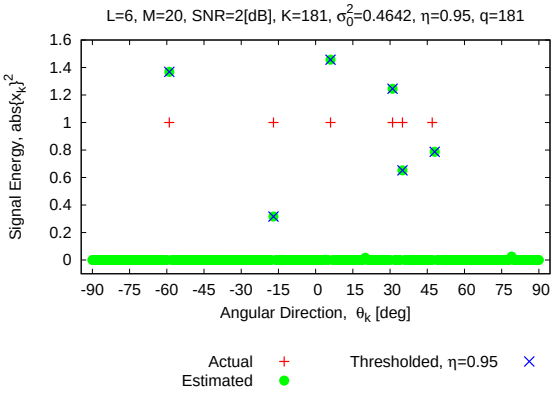

(a) $RMSE_\theta = 0.41\ \ [deg]$

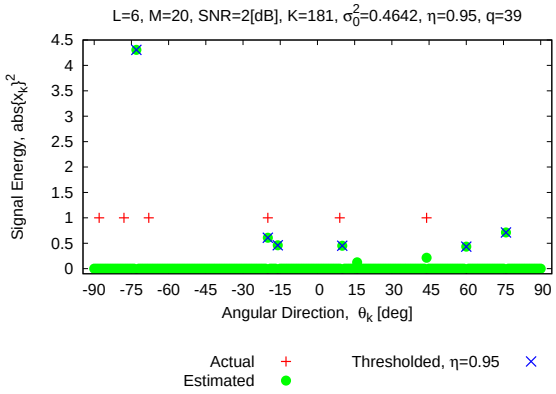

(b) $RMSE_\theta = 46.58\ \ [deg]$

$\widetilde{L} > L$

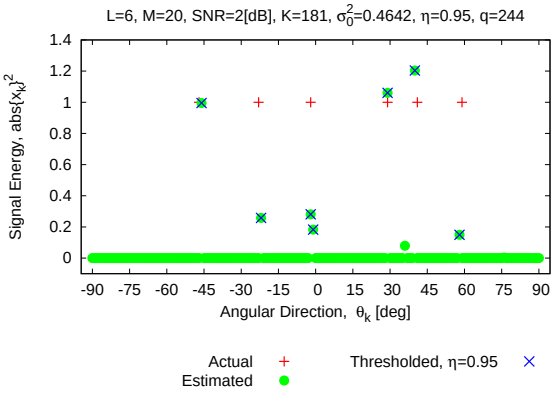

(c) $RMSE_\theta = 0.91\ \ [deg]$

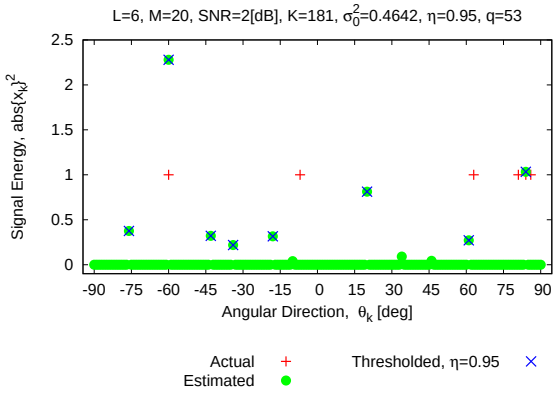

(d) $RMSE_\theta = 50.58\ \ [deg]$

$\widetilde{L} < L$

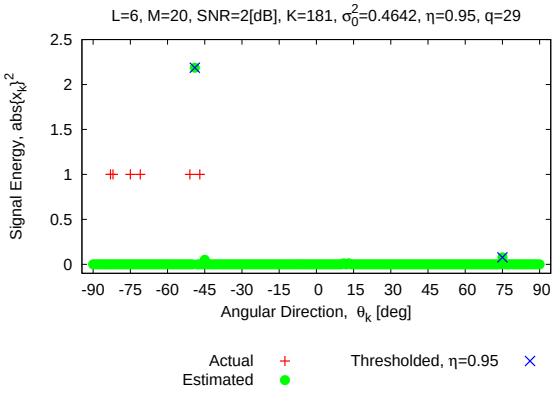

(e) $RMSE_\theta = 155.18\ \ [deg]$

Figure 5: *BCS DoA estimation examples*: (a) $\widetilde{L} = L$ with low $RMSE_\theta$, (b) $\widetilde{L} = L$ with high $RMSE_\theta$, (c) $\widetilde{L} > L$ with low $RMSE_\theta$, (d) $\widetilde{L} > L$ with high $RMSE_\theta$ and (e) $\widetilde{L} < L$ with high $RMSE_\theta$ (in this case it is impossible to obtain a low $RMSE_\theta$).

Performances analysis

GOAL: this section is aimed to analyzing the performances of the BCS method in terms of $RMSE$ and PL. The $RMSE$ has been computed considering two cases:

- the number of signals is not known
- the number of signals in known

0.0.1 Performances vs the SNR

Simulation Parameters

- Scenario
  - BPSK signals ($E_l^{inc} \in \{-1, 1\}$)
  - Number of incident signals: $L = 2$
  - Signal directions: $\underline{\theta} = \{0, 7\}\ [deg]$
  - **Signal to noise ratio:** $SNR = [-5, 20]\ dB$
- Array parameters
  - Elements spacing: $d = 0.5\lambda$
  - Number of elements: $M = 10$
- BCS parameters
  - Number of angular locations: $K = 181$
  - $\sigma_0^2 = 4.642 \times 10^{-1}$
- Simulation
  - Number of independent realizations $Q = 100$ (the noise and the signal amplitudes are random, while the DoAs are fixed)

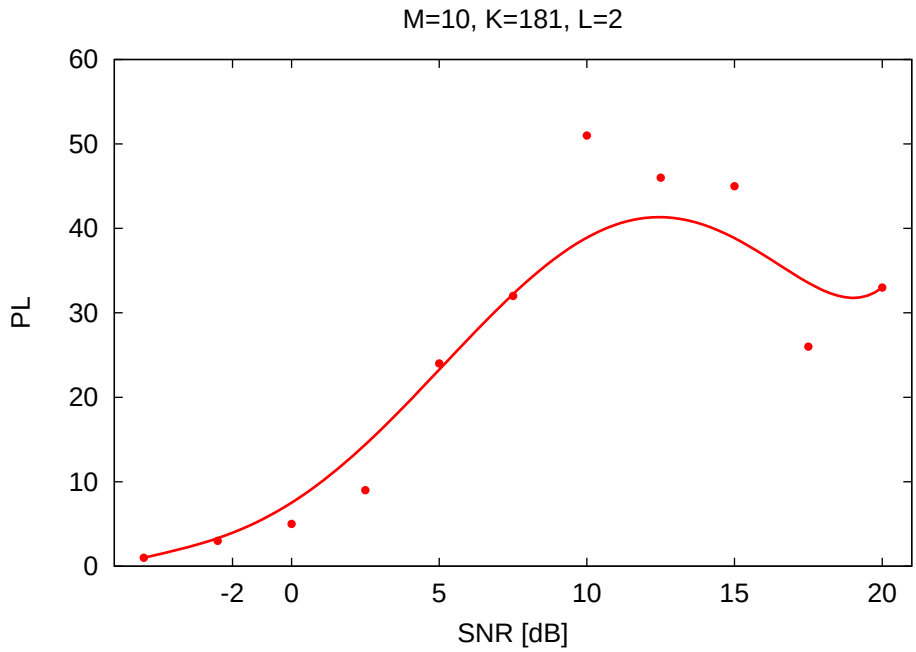

(a)

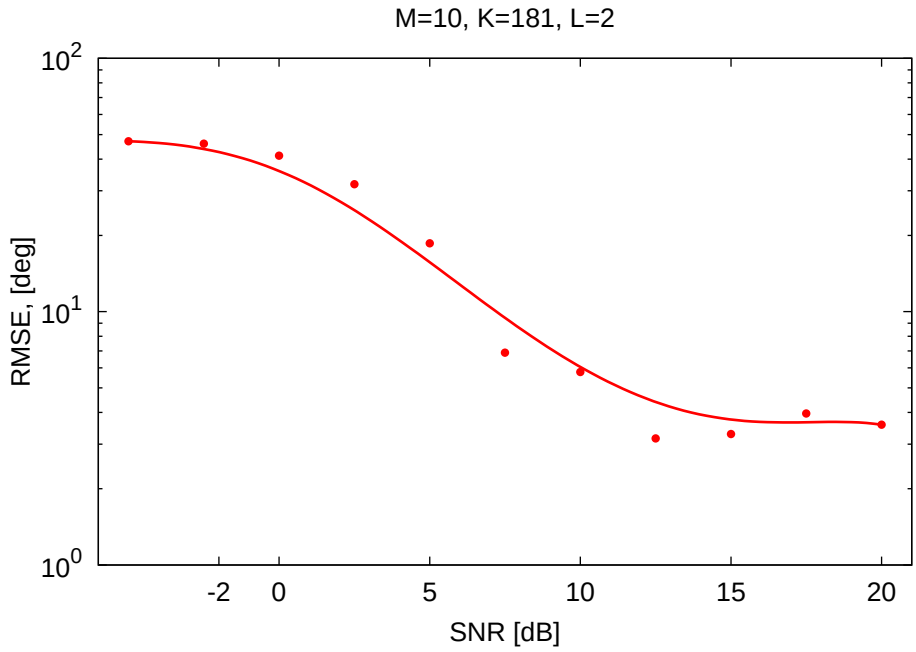

(b)

Figure 6: *BCS performances analysis:* (a) P_L and (b) $RMSE$ vs the SNR value (L is unknown).

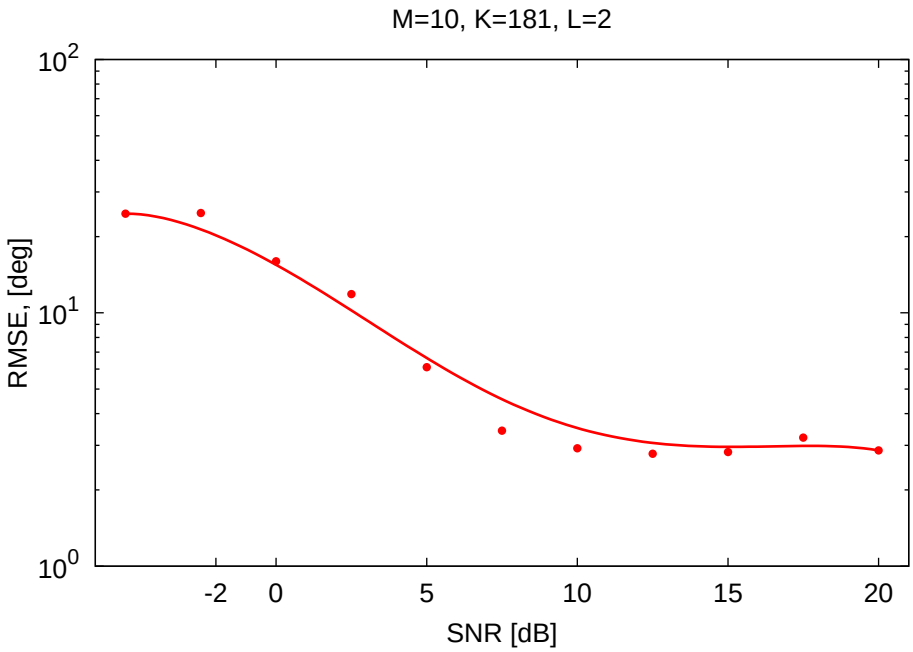

Figure 7: *BCS performances analysis:* $RMSE$ vs the SNR value (L is known).

Performances vs the number of array elements M

Simulation Parameters

- Scenario
  - BPSK signals ($E_l^{inc} \in \{-1, 1\}$)
  - Number of incident signals: $L = 2$
  - Signal directions: $\underline{\theta} = \{0, 7\}$ $[deg]$
  - Signal to noise ratio: $SNR = 7$ dB
- Array parameters
  - Elements spacing: $d = 0.5\lambda$
  - **Number of elements:** $M \in [5, 30]$
- BCS parameters
  - Number of angular locations: $K = 181$
  - $\sigma_0^2 = 4.642 \times 10^{-1}$
- Simulation
  - Number of independent realizations $Q = 100$ (the noise and the signal amplitudes are random, while the DoAs are fixed)

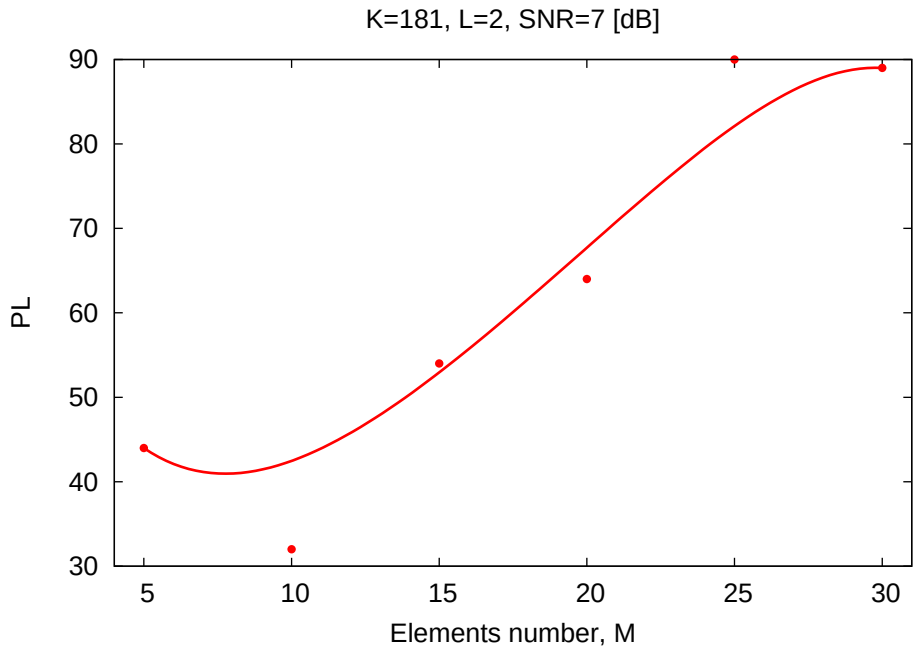

(a)

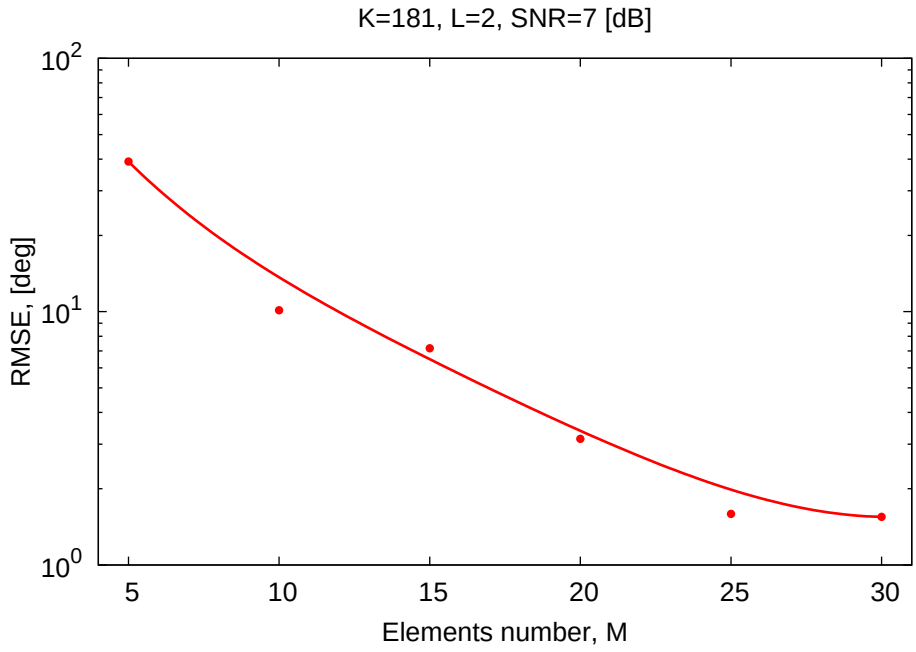

(b)

Figure 8: *BCS performances analysis:* (a) P_L and (b) $RMSE$ vs the number of array elements M (L is unknown).

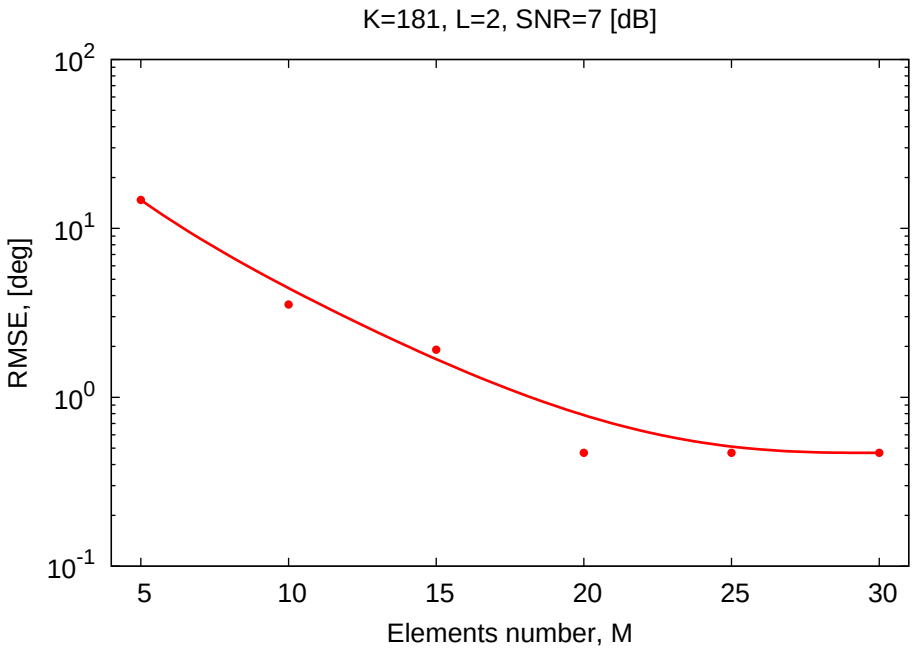

Figure 9: *BCS performances analysis:* $RMSE$ vs vs the number of array elements M (L is known).

Performances vs the number of incident signals L

Simulation Parameters

- Scenario
  - BPSK signals ($E_l^{inc} \in \{-1, 1\}$)
  - **Number of incident signals:** $L \in [1, 7]$
  - **Signal directions:**

L	θ_1	θ_2	θ_3	θ_4	θ_5	θ_6	θ_7
1	0	-	-	-	-	-	-
2	0	7	-	-	-	-	-
3	0	7	-12	-	-	-	-
4	0	7	-12	-24	-	-	-
5	0	7	-12	-24	45	-	-
6	0	7	-12	-24	45	75	-
7	0	7	-12	-24	45	75	-33

Table 1: Signal directions for different numbers of signals.

  - Signal to noise ratio**:** $SNR = 7\ dB$
- Array parameters
  - Elements spacing: $d = 0.5\lambda$
  - Number of elements: $M = 10$
- BCS parameters
  - Number of angular locations: $K = 181$
  - $\sigma_0^2 = 4.642 \times 10^{-1}$
- Simulation
  - Number of independent realizations $Q = 100$ (the noise and the signal amplitudes are random, while the DoAs are fixed)

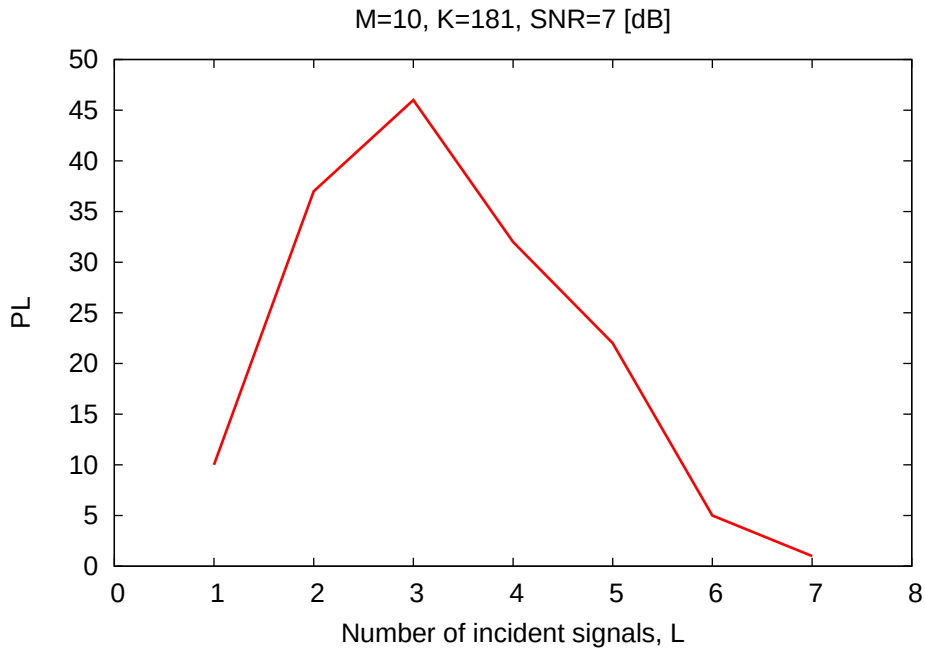

(a)

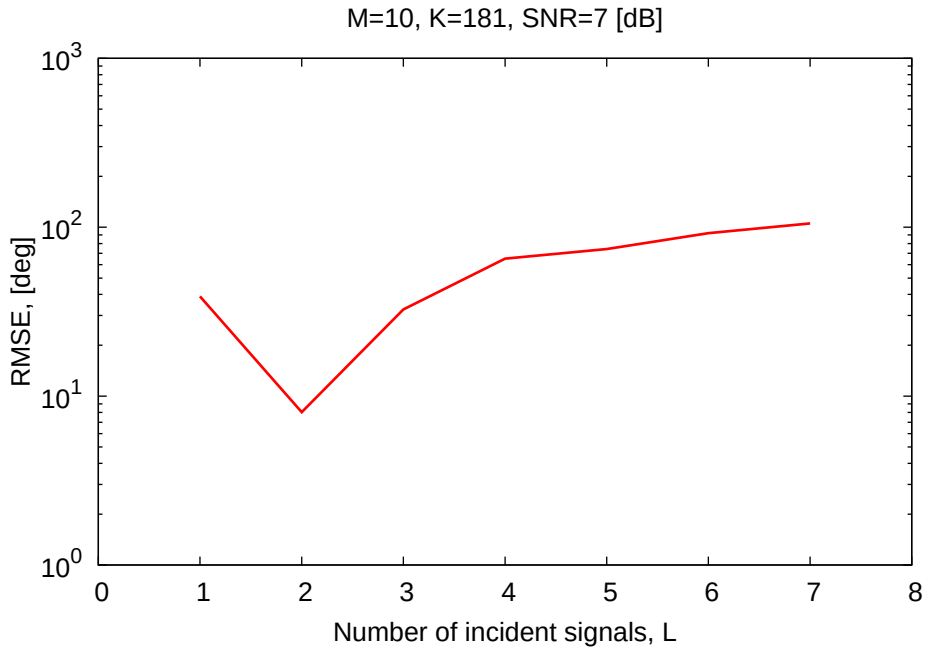

(b)

Figure 10: *BCS performances analysis:* (a) P_L and (b) $RMSE$ vs the number of incident signals L (L is unknown).

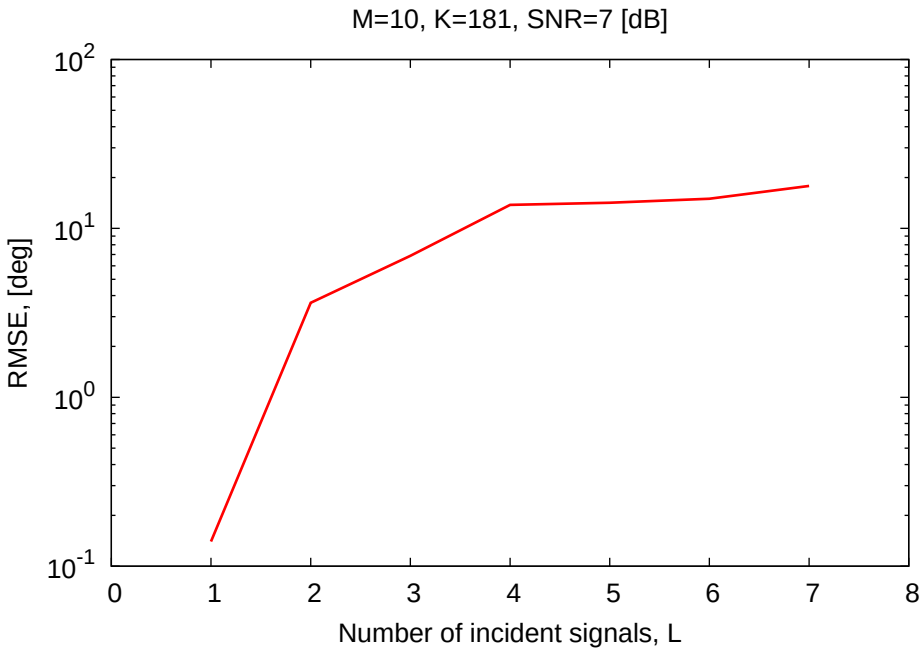

Figure 11: *BCS performances analysis: RMSE* vs the number of incident signals L (L is known).

Performances vs the signal spacing $\Delta\theta$

Simulation Parameters

- Scenario
  - BPSK signals ($E_l^{inc} \in \{-1, 1\}$)
  - Number of incident signals: $L = 2$
  - **Signals spacing**: $\Delta\theta^{l(l+1)} \in [2, 20]\ deg$
  - **Signals directions**: $\underline{\theta} = \left\{-\frac{\Delta\theta^{l(l+1)}}{2}, \frac{\Delta\theta^{l(l+1)}}{2}\right\}\ [deg]$
  - Signal to noise ratio**:** $SNR = 7\ dB$
- Array parameters
  - Elements spacing: $d = 0.5\lambda$
  - Number of elements: $M = 10$
- BCS parameters
  - Number of angular locations: $K = 181$
  - $\sigma_0^2 = 4.642 \times 10^{-1}$
- Simulation
  - Number of independent realizations $Q = 100$ (the noise and the signal amplitudes are random, while the DoAs are fixed)

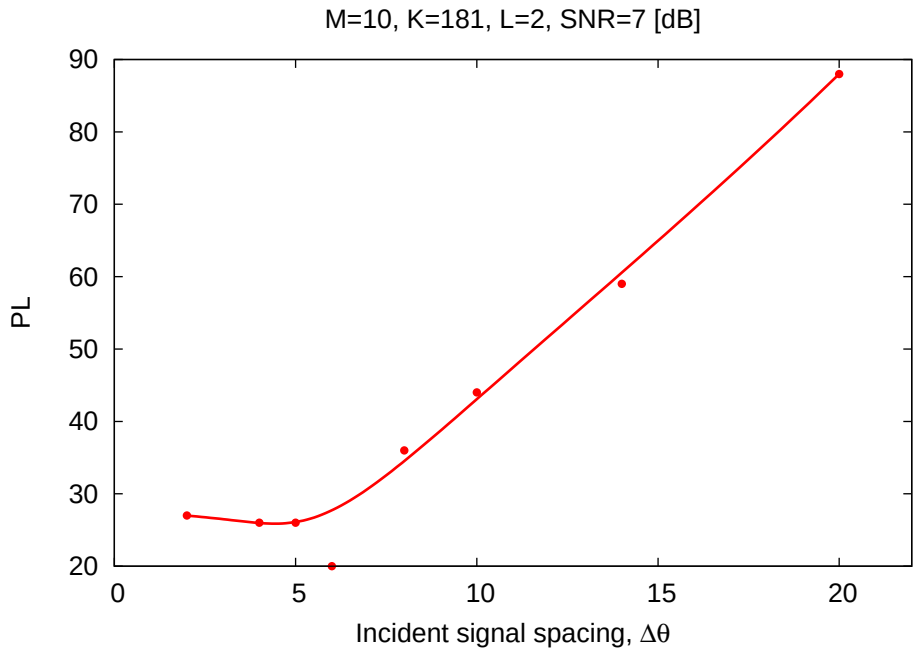

(a)

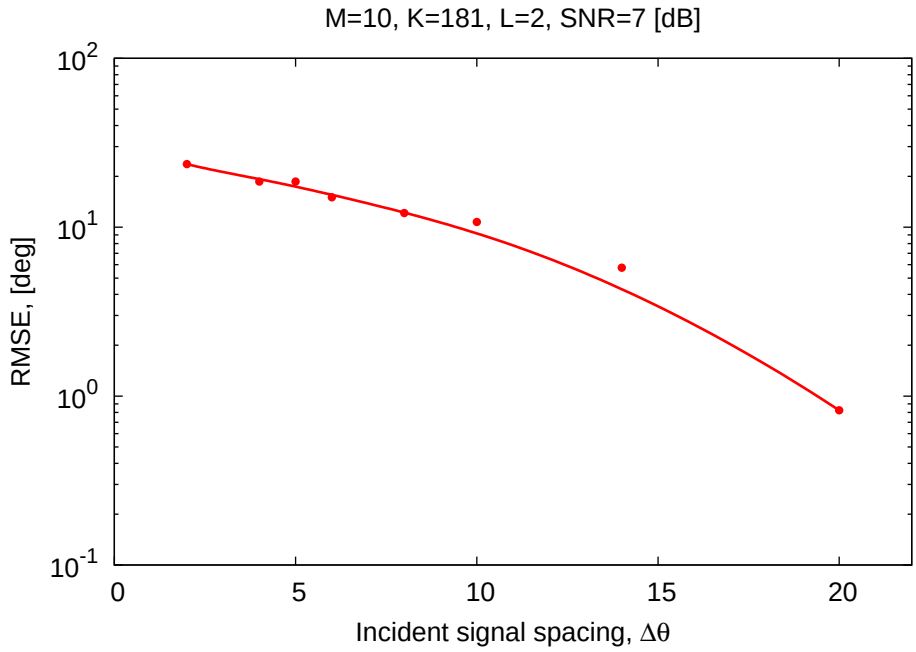

(b)

Figure 12: *BCS performances analysis:* (a) P_L and (b) $RMSE$ vs the distance between incident signals (L is unknown).

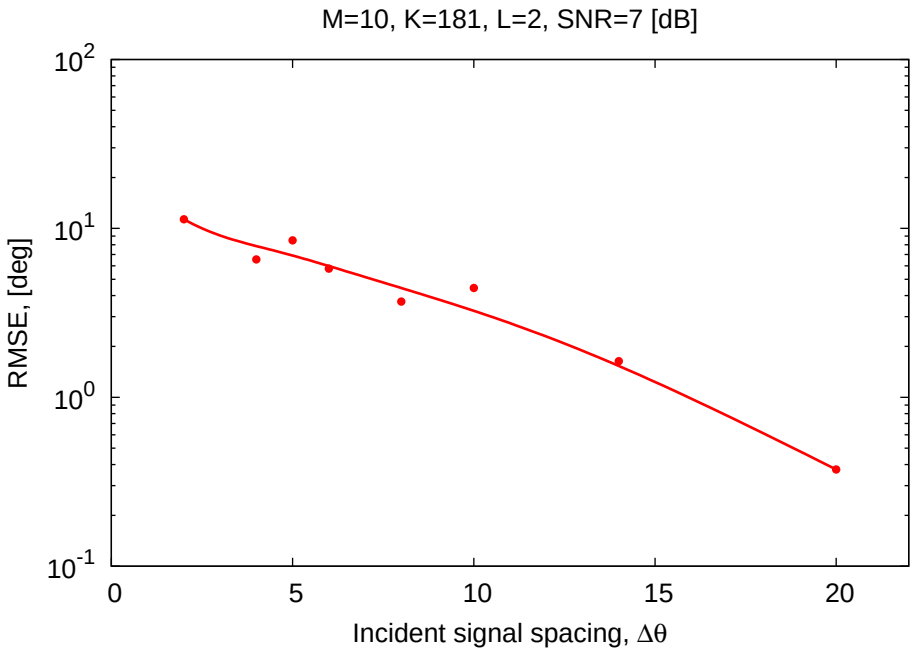

Figure 13: *BCS performances analysis:* $RMSE$ vs the distance between incident signals (L is known).

Single Snapshot Comparison with ESPRIT

Analysis of the performances of the algorithm when only $W = 1$ snapshot is considered

The objective of this section is to compare the performance of the proposed method with the performances of the ESPRIT method. In order to compare the two methods under the same conditions, the DoA estimation is performed only from one snapshot. As it can be noticed, the ESPRIT method does not work with just one snapshot.

Case 01: signals DoAs locked to the BCS grid In the following example the directions of arrival of the impinging signals are locked to the user-defined grid used by the BCS solver.

- Scenario
  - $L = 2$
  - $\underline{\theta} = \{0, 7\}$ $[deg]$
  - BPSK signals
  - $SNR \in [0, 20]$ dB (def. Imaging)
- Array
  - $M = \{10, 25\}$
  - $d = 0.5\lambda$
  - $W = 1$
- Method
  - $\sigma_0^2 = 4.642 \times 10^{-1}$
  - $K = 181$
- Simulation
  - $Q = 200$ independent realizations

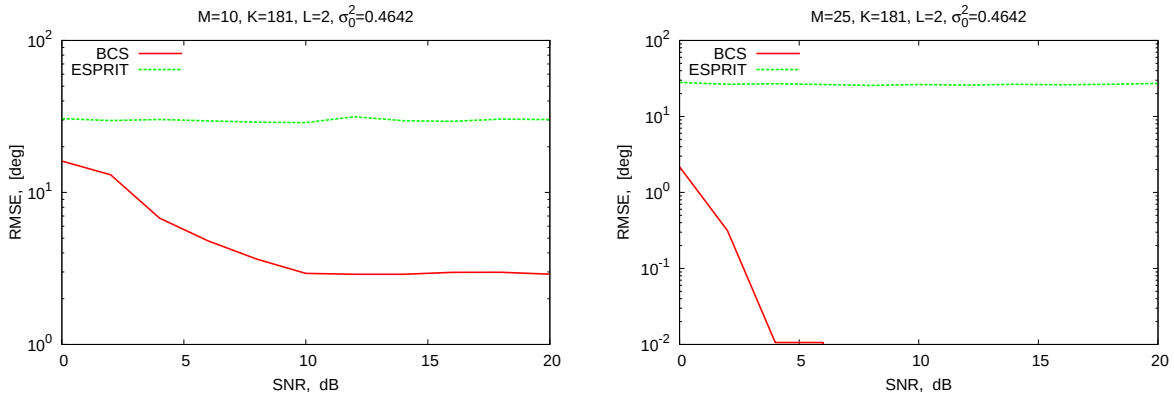

(a) (b)

Figure 14: $RMSE$ vs SNR when only $W = 1$ snapshots are acquired. As it can be observed, compared to BCS, the performances of $ESPRIT$ are very poor.

Case 02: free signals DoAs In the following example the direction of arrival of the incident signals are not locked to the BCS solver grid.

- Scenario
  - $L = 2$
  - $\underline{\theta} = \{0, 7\}$ $[deg]$
  - BPSK signals
  - $SNR \in [0, 20]$ dB (def. Imaging)
- Array
  - $M = \{10, 25\}$
  - $d = 0.5\lambda$
  - $W = 1$
- Method
  - $\sigma_0^2 = 4.642 \times 10^{-1}$
  - $K = 181$
- Simulation
  - $Q = 200$ independent realizations

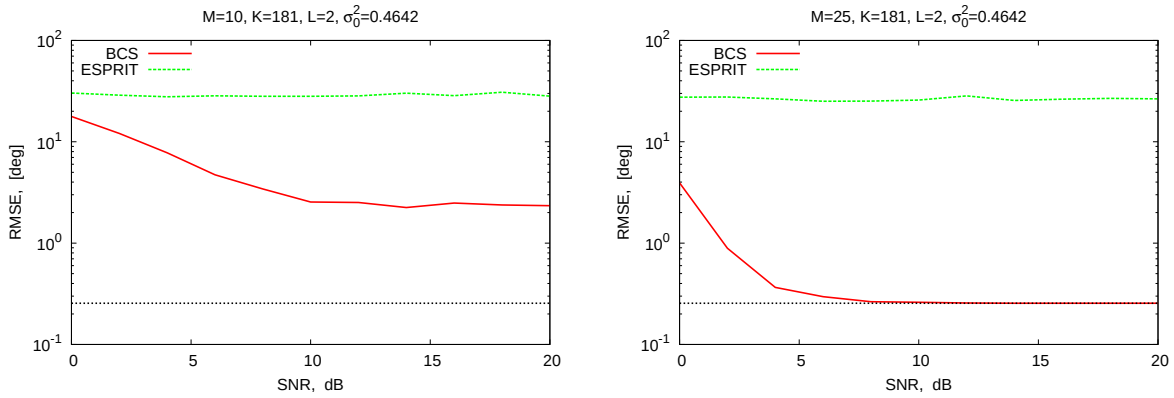

(a) (b)

Figure 15: $RMSE$ vs SNR when only $W = 1$ snapshots are acquired. As it can be observed, compared to BCS, the performances of $ESPRIT$ are very poor. The black curve represents the minimum achievable error, which in this specific case is equal to $RMSE_{min} = \sqrt{\frac{[(0.3)^2+(0.2)^2]}{2}} \simeq 2.55 \times 10^{-1}$ $[deg]$.

References

[1] M. Carlin, P. Rocca, G. Oliveri, F. Viani, and A. Massa, "Directions-of-arrival estimation through Bayesian Compressive Sensing strategies," IEEE Trans. Antennas Propag., vol. 61, no. 7, pp. 3828-3838, Jul. 2013.

[2] M. Carlin, P. Rocca, G. Oliveri, and A. Massa, "Bayesian compressive sensing as applied to directions-of-arrival estimation in planar arrays," Journal of Electrical and Computer Engineering, Special Issue on "Advances in Radar Technologies", vol. 2013, pp. 1-12, 2013.

[3] M. Carlin, P. Rocca, "A Bayesian compressive sensing strategy for direction-of-arrival estimation," 6th European Conference on Antennas Propag. (EuCAP 2012), Prague, Czech Republic, pp. 1508-1509, 26-30 Mar. 2012.

[4] L. Lizzi, F. Viani, M. Benedetti, P. Rocca, and A. Massa, "The M-DSO-ESPRIT method for maximum likelihood DoA estimation," Progress in Electromagnetic Research, vol. 80, pp. 477-497, 2008.

[5] M. Donelli, F. Viani, P. Rocca, and A. Massa, "An innovative multi-resolution approach for DoA estimation based on a support vector classification," IEEE Trans. Antennas Propag., vol. 57, no. 8, pp. 2279-2292, Aug. 2009.

[6] L. Lizzi, G. Oliveri, P. Rocca, and A. Massa, "Estimation of the direction-of-arrival of correlated signals by means of a SVM-based multi-resolution approach," IEEE Antennas Propag. Society International Symposium (APSURSI), Toronto, ON, Canada, pp. 1-4, 11-17 Jul. 2010.

[7] A. Massa, P. Rocca, and G. Oliveri, "Compressive sensing in electromagnetics - A review," IEEE Antennas and Propagation Magazine, pp. 224-238, vol. 57, no. 1, Feb. 2015.

[8] G. Oliveri and A. Massa, "Bayesian compressive sampling for pattern synthesis with maximally sparse non-uniform linear arrays," IEEE Trans. Antennas Propag., vol. 59, no. 2, pp. 467-481, Feb. 2011.

[9] G. Oliveri, M. Carlin, and A. Massa, "Complex-weight sparse linear array synthesis by Bayesian Compressive Sampling," IEEE Trans. Antennas Propag., vol. 60, no. 5, pp. 2309-2326, May 2012.

[10] G. Oliveri, P. Rocca, and A. Massa, "Reliable diagnosis of large linear arrays - A Bayesian Compressive Sensing approach," IEEE Trans. Antennas Propag., vol. 60, no. 10, pp. 4627-4636, Oct. 2012.

[11] F. Viani, G. Oliveri, and A. Massa, "Compressive sensing pattern matching techniques for synthesizing planar sparse arrays," IEEE Trans. Antennas Propag., vol. 61, no. 9, pp. 4577-4587, Sept. 2013.

[12] G. Oliveri, E. T. Bekele, F. Robol, and A. Massa, "Sparsening conformal arrays through a versatile BCS-based method," IEEE Trans. Antennas Propag., vol. 62, no. 4, pp. 1681-1689, Apr. 2014.

[13] M. Carlin, G. Oliveri, and A. Massa, "Hybrid BCS-deterministic approach for sparse concentric ring isophoric arrays," IEEE Trans. Antennas Propag., vol. 63, no. 1, pp. 378-383, Jan. 2015.

[14] G. Oliveri, N. Anselmi, and A. Massa, "Compressive sensing imaging of non-sparse 2D scatterers by a total-variation approach within the Born approximation," IEEE Trans. Antennas Propag., vol. 62, no. 10, pp. 5157-5170, Oct. 2014.

[15] L. Poli, G. Oliveri, and A. Massa, "Imaging sparse metallic cylinders through a Local Shape Function Bayesian Compressive Sensing approach," Journal of Optical Society of America A, vol. 30, no. 6, pp. 1261-1272, 2013.

[16] F. Viani, L. Poli, G. Oliveri, F. Robol, and A. Massa, "Sparse scatterers imaging through approximated multitask compressive sensing strategies," Microwave Opt. Technol. Lett., vol. 55, no. 7, pp. 1553-1558, Jul. 2013.

[17] L. Poli, G. Oliveri, P. Rocca, and A. Massa, "Bayesian compressive sensing approaches for the reconstruction of two-dimensional sparse scatterers under TE illumination," IEEE Trans. Geosci. Remote Sensing, vol. 51, no. 5, pp. 2920-2936, May 2013.

[18] L. Poli, G. Oliveri, and A. Massa, "Microwave imaging within the first-order Born approximation by means of the contrast-field Bayesian compressive sensing," IEEE Trans. Antennas Propag., vol. 60, no. 6, pp. 2865-2879, Jun. 2012.

[19] G. Oliveri, P. Rocca, and A. Massa, "A bayesian compressive sampling-based inversion for imaging sparse scatterers," IEEE Trans. Geosci. Remote Sensing, vol. 49, no. 10, pp. 3993-4006, Oct. 2011.

[20] G. Oliveri, L. Poli, P. Rocca, and A. Massa, "Bayesian compressive optical imaging within the Rytov approximation," Optics Letters, vol. 37, no. 10, pp. 1760-1762, 2012.

[21] L. Poli, G. Oliveri, F. Viani, and A. Massa, "MT-BCS-based microwave imaging approach through minimum-norm current expansion," IEEE Trans. Antennas Propag., vol. 61, no. 9, pp. 4722-4732, Sep. 2013.